Imipramine as an alternative to formamide to detubulate rat ventricular cardiomyocytes

Aurelia Bourcier, Marion Barthe, Ibrahim Bedioune, Patrick Lechêne, Hela Ben Miled, Grégoire Vandecasteele, Rodolphe Fischmeister, Jérôme Leroy

IMIPRAMINE AS AN ALTERNATIVE TO FORMAMIDE TO DETUBULATE RAT VENTRICULAR CARDIOMYOCYTES

AURELIA BOURCIER[1], MARION BARTHE*[1], IBRAHIM BEDIOUNE*[1], PATRICK LECHÊNE*[1], HELA BEN MILED[1], GRÉGOIRE VANDECASTEELE[1], RODOLPHE FISCHMEISTER[1] AND JÉRÔME LEROY[1]

[1]INSERM UMR-S 1180, FACULTE DE PHARMACIE, UNIV. PARIS-SUD, UNIVERSITE PARIS-SACLAY, F-92296, CHATENAY-MALABRY, FRANCE.

*These authors contributed equally to present study

Running title: Imipramine as a detubulating agent for cardiac myocytes

Correspondence to:

Jérôme LEROY

INSERM UMR-S1180, LabEx LERMIT, DHU TORINO

UNIV. PARIS-SUD, UNIVERSITE PARIS-SACLAY,

Faculté de Pharmacie

5, Rue J.-B. Clément
F-92296 Châtenay-Malabry Cedex

France

Tel. 33-1-46 83 57 71

Fax 33-1-46 83 54 75

E-mail: jerome.leroy@u-psud.fr

NEW FINDINGS

What is the central question of this study?

Cardiac T-tubules are membrane invaginations essential for the excitation-contraction coupling. Imipramine, an antidepressant agent, is a cationic amphiphilic drug which interferes with the PI(4,5)P2 interactions with proteins maintaining the tubular system, but its validation as a new detubulating tool as not yet been reported.

What is the main finding and its importance?

We validate imipramine as a more efficient and less toxic detubulating agent of cardiomyocytes, than formamide, provide new insights on how PI(4,5)P2 is crucial to maintain T-tubules attached to the cell surface and on the cardiotoxic effects of imipramine overdoses.

ABSTRACT

Cardiac T-tubules are membrane invaginations essential for the excitation-contraction coupling (ECC). Imipramine like other cationic amphiphilic drugs, interfere with the $PI(4,5)P_2$ interactions with proteins maintaining the tubular system connected to cell surface. Our main purpose was to validate imipramine as a new detubulating agent in cardiomyocytes. Staining adult rat ventricular myocytes (ARVMs) with di-4-ANEPPS, we showed that unlike formamide, imipramine induces a complete detubulation with no impact on cell viability. Using the patch-clamp technique, we observed a ~40% decrease in cell capacitance after imipramine pretreatment and a reduction of $I_{Ca,L}$ amplitude by ~72%. These parameters were not affected in atrial cells, excluding direct side effects of imipramine. The β-adrenergic receptor's (β-AR) stimulation of the remaining $I_{Ca,L}$ with isoproterenol (Iso) was still effective. ECC was investigated in ARVMs loaded with Fura-2 and paced at 1 Hz, allowing simultaneous measurement of Ca^{2+} transient (CaT) and sarcomere shortening (SS). Amplitude of both CaT and SS was decreased by imipramine and partially restored by Iso. Furthermore, detubulated cells exhibited Ca^{2+} homeostasis perturbations. Real-time cAMP variations induced by Iso using a Förster resonance energy transfer (FRET) biosensor revealed a ~27% decreased cAMP elevation upon β-AR stimulation.To conclude, we validated a new cardiomyocyte detubulation method using imipramine which is more efficient and less toxic than formamide. This antidepressant agent induces the hallmark effects of detubulation on ECC and its β-AR stimulation. Besides, we provide new insights on how imipramine overdose may affect cardiac function and suggest that $PI(4,5)P_2$ is crucial to maintain T-tubules structure.

INTRODUCTION

Transverse tubules (T-tubules) of cardiac myocytes are invaginations of the surface membrane that form a complex interconnected network penetrating deep into the cell interior (Hong & Shaw, 2017). These tubular structures are found mostly in ventricular myocytes where they occur near the sarcomeric z-discs (Caldwell *et al.*, 2014), allowing functional junction with the sarcoplasmic reticulum called dyad. They are critical for the excitation-contraction coupling (ECC) by concentrating L-type Calcium channels (LTCC) and positioning them at close proximity of ryanodine receptors (RyR) clusters at the junction of sarcoplasmic reticulum. During an action potential, T-tubules propagate the cell-membrane depolarization inside the cell allowing Ca^{2+} entry to trigger successive Ca^{2+} release thus promoting synchronicity as well as efficiency of the Ca^{2+}-induced Ca^{2+} release (CICR) phenomenon (Fu *et al.*, 2016). Their enrichment with ion channels and the presence of signaling pathways components such as β-adrenergic receptors (β-AR) (Nikolaev *et al.*, 2010) and adenylyl cyclases (AC) (Timofeyev *et al.*, 2013) make these structures essential for cardiomyocyte function and regulation. Alterations in their morphology and density are believed to take part in the development of heart failure (Hong & Shaw, 2017), thus understanding their role is crucial and may open new therapeutic avenues.

To define the role of the T-tubules in the physiology of ventricular cells, the Orchard's group in the late 90's provided a simple detubulation method. It is based on an osmotic shock induced by a high concentration of formamide and its quick removal to disrupt the normal coupling of the membrane invaginations with the cell surface (Kawai *et al.*, 1999; Brette *et al.*, 2002). Since then, dozens of reports were published using this technique as a gold standard method to detubulate cardiomyocytes. However, despite the apparent preservation of the microtubule network (Brette *et al.*, 2002), formamide incubation and removal produce drastic changes in cell volume (Kawai *et al.*, 1999) which may alter subcellular microdomains. Furthermore, although quite efficient, detubulation by formamide is incomplete, with ~20% of the cells remaining intact (Kawai *et al.*, 1999; Pasek *et al.*, 2008). Additionally, ~80% of the myocytes still exhibit a faint staining of invaginations (Brette *et al.*, 2002). More importantly, formamide-induced detubulation is generally variable and more importantly is accompanied with the loss of a large proportion of viable cells which is especially prejudicial when performed on cardiac cells isolated from valuable pathological or genetically modified models. Therefore, an alternative treatment which would be more efficient and less toxic would be useful for cardiac physiologists. Interestingly, a recent study demonstrated that high concentrations of cationic amphiphilic drugs (CADs) can produce detubulation of adult rat ventricular myocytes (ARVMs) probably by interfering with $PI(4,5)P_2$ interactions with cytoskeletal and BAR (Bin-Amphiphysin-Rvs) domain containing proteins (Osman *et al.*, 2016). However, a comparison of this detubulation method with the formamide-induced removal of T-tubules has not yet been

performed and the consequences on CICR or β-AR signaling of the detubulation induced by CADs binding to $PI(4,5)P_2$ in ventricular myocytes are unknown. Our aim here was therefore to provide these informations. To do so, we selected one of the CADs causing cardiomyocyte detubulation, an antidepressant agent named imipramine (Osman *et al.*, 2016).

METHODS

Ethical approval

All experiments were carried out according to the European Community guiding principles in the care and use of animals (2010/63/UE, 22 September 2010), the local Ethics committee (CEEA26 CAPSud) guidelines and the French decree n°2013-118, 1st February 2013 on the protection of animals used for scientific purposes (JORF n°0032, 7 February 2013 p2199, text n°24). Animal experiments were approved by the French Ministry of Agriculture (prefectural agreement N°2016-108 and agreement to our animal facility N° C 92-019-01). Rats had ad libitum access to water and standard rat chow and were housed in a well-ventilated, specific pathogen-free, temperature-controlled environment to ensure that animals were not under stress. Enrichment was added in animal cages.

Reagents

Isoproterenol from Sigma-Aldrich (Saint-Quentin, France) was prepared in a 1 mg/mL ascorbic acid solution at 10 mM (Sigma-Aldrich, Saint-Quentin, France). Di-4-ANEPPS (Pyridinium, 4-(2-(6-(dibutylamino)-2-naphthalenyl)ethenyl)-1-(3-sulfopropyl)-, hydroxide), formamide and imipramine were from Sigma-Aldrich, Saint-Quentin, France).

Cardiomyocyte isolation and culture

Male Wistar rats (250–300 g) were anesthetized by intraperitoneal injection of pentobarbital (0.1 mg/g) and hearts were excised rapidly. Individual ARVMs were obtained by retrograde perfusion of the heart as previously described (Mika *et al.*, 2013). For enzymatic dissociation, the hearts were perfused at a constant flow of 6 mL/min at 37 °C with a Ca^{2+}-free Ringer solution containing (in mM): NaCl 117, KCl 5.7, $NaHCO_3$ 4.4, KH_2PO_4 1.5, $MgCl_2$ 1.7, D-glucose 11.7, Na_2-phosphocreatine 10, taurine 20, and 4-(2-hydroxyethyl)piperazine-1-ethanesulfonic acid (HEPES) 21, pH 7.1 during 5 min, followed by a perfusion at 4 mL/min for 40 min with the same solution containing 1 mg/mL of collagenase A (Roche Diagnostics GmbH, Mannheim, Germany) plus 300 µM ethylene glycol tetraacetic acid (EGTA) and $CaCl_2$ to adjust free Ca^{2+} concentration to 20 µM. The ventricles and atria were then separated, finely chopped and gently agitated to dissociate individual cells from each tissue. The resulting cell suspension was filtered on gauze and the cells were allowed to settle down. The supernatant was discarded and cells resuspended four more times with Ringer solution at

increasing [Ca^{2+}] from 20 to 300 µM. Freshly isolated cells were suspended in minimal essential medium (MEM: M 4780; Sigma, St Louis, MO, USA) containing 1.2 mM [Ca^{2+}] supplemented with 2.5% foetal bovine serum (FBS, Invitrogen, Cergy-Pontoise, France), 1% penicillin–streptomycin (P-S), 20 mM HEPES (pH 7.6), and plated on 35 mm, laminin-coated (10 mg/mL) culture dishes at a density of 10^4 cells per dish and kept at 37°C (0.5% CO_2). After 1 h, the medium was replaced by 300 µL of FBS-free MEM. To perform FRET imaging, the medium was replaced by 300 µL of FCS-free MEM or transduced with an adenovirus encoding the Epac-S^{H187} FRET-based sensor (Klarenbeek *et al.*, 2015) at a multiplicity of infection (MOI) of 1000 pfu/cell and cells were cultured for 24h prior to the experiments. All patch-clamp and IonOptix experiments were performed on freshly isolated cardiomyocytes after at least 1h FBS deprivation.

Electrophysiological experiments

The whole cell configuration of the patch-clamp technique was used to record $I_{Ca,L}$. Patch electrodes resistance between 0.5–1.5 MΩ when filled with internal solution containing (in mM): CsCl 118, EGTA 5, $MgCl_2$ 4, Na_2-phosphocreatine 5, Na_2ATP 3.1, Na_2GTP 0.42, $CaCl_2$ 0.062 (pCa 8.5), HEPES 10, adjusted to pH 7.3. External Cs^+-Ringer solution contained (in mM): NaCl 107.1, CsCl 20, $NaHCO_3$ 4, NaH_2PO_4 0.8, D-glucose 5, sodium pyruvate 5, HEPES 10, $MgCl_2$ 1.8, $CaCl_2$ 1.8 adjusted to pH 7.4. The cells were depolarized every 8 s from –50 mV to 0 mV during 400 ms. The junction potential was adjusted to give zero current between pipette and bath solution before the cells were attached to obtain a tight gigaseal (>1GΩ). Cell capacitance was obtained by fitting the transient portion of the current response to a 5 mV pulse from -80 mV with a single exponential and calculated from the exponential and the area under the curve obtained. The use of –50 mV as holding potential allowed the inactivation of voltage-dependent sodium currents. Currents were not compensated for capacitance and leak currents. The amplitude of $I_{Ca,L}$ was measured as the difference between the peak inward current and the current at the end of the depolarization pulses. The current-voltage relationship and steady-state inactivation properties were measured by applying a 200 ms pulse varying from -60 to +60 mV, followed by a 3 ms repolarization to -50 mV before the 200 ms test pulse to 0 mV. The current density-voltage (*I*-*V*) relationships were fitted with a modified Boltzmann equation as follows: $I=G_{max}x(V-V_{rev})/(1+exp(-(V- V_{0.5,act})/k))$, where *I* is the current density (in pA/pF), G_{max} is the maximum conductance (in nS/pF), V_{rev} is the reversal potential (in mV), $V_{0.5,act}$ is the midpoint voltage for current activation (in mV), and *k* is the slope factor (in mV). Steady-state inactivation curves were obtained by normalizing the peak current at each test potential to the maximal current, and fitted with a Boltzmann equation: $I/I_{max} = (1-A)/\{1+exp[(V-V_{0.5,\ inact})/k]\}+A$, where $V_{0.5,inact}$ is the potential of half-maximal inactivation, *k* is the slope factor, *A* is the amplitude of the non-inactivating $I_{Ca,L}$ current. The cells were voltage-clamped using patch-clamp amplifiers: either a RK-400 (Bio-Logic, Claix, France) or an Axopatch 200B patch clamp amplifier (Axon Instruments,

Inc., Union City, CA, USA). Currents were analogue filtered at 5 KHz and digitally sampled at 10 KHz using a 16-bit analogue-to-digital converter (DT321; Data translation, Marlboro, MA, USA or a digidata 1440A, Axon Instruments) connected to a PC (Dell, Austin, Texas, USA).

Measurements of Ca^{2+} transients and sarcomere shortening

All experiments were performed at room temperature. Isolated ARVMs were loaded with 1 µM Fura-2 AM (Invitrogen) and pluronic acid (0.012%, Molecular Probes) for 15 min in a Ringer solution containing (in mM): KCl 5.4; NaCl 121.6; Na-pyruvate 5; $NaHCO_3$ 4.013; NaH_2PO_4 0.8; $CaCl_2$ 1.8; $MgCl_2$ 1.8; glucose 5 and HEPES 10 (pH 7,4 with NaOH). Sarcomere shortening and Fura-2 ratio (measured at 512 nm upon excitation at 340 and 380 nm) were simultaneously recorded in Ringer solution, using a double excitation spectrofluorimeter coupled with a video detection system (IonOptix, Milton, MA, USA). Myocytes were electrically stimulated with biphasic field pulses (5 V, 4 ms) at a frequency of 1 Hz as previously described (Mika *et al.*, 2013). Ca^{2+} transient amplitude was measured by dividing the twitch amplitude (difference between the end-diastolic and the peak systolic ratios) by the end-diastolic ratio, thus corresponding to the percentage of variation in the Fura-2 ratio. Similarly, sarcomere shortening was assessed by its percentage of variation, which is obtained by dividing the twitch amplitude (difference between the end-diastolic and the peak systolic sarcomere length) by the end-diastolic sarcomere length. Relaxation kinetics were estimated by a non-linear fit of the decaying part of the Ca^{2+} transient and sarcomere shortening traces with the following equation: $X(t)=A*\exp(-(t-t_0)/\tau))+A_0$, where t_0 is zero time, A_0 the asymptote of the exponential, A the relative amplitude of the exponential, and τ the time constant of relaxation. The maximum first derivative of transients during the deflexion allowed to determine the rising velocities of the signals. All parameters were calculated offline on a dedicated software (IonWizard 6×, IonOptix®).

FRET imaging

FRET experiments were performed at room temperature 24h after cell plating. Cells were maintained in a Ringer solution containing (in mM): NaCl 121.6, KCl 5.4, $MgCl_2$ 1.8; $CaCl_2$ 1.8; $NaHCO_3$ 4, NaH_2PO_4 0.8, D-glucose 5, sodium pyruvate 5, HEPES 10, adjusted to pH 7.4 (with NaOH). Images were captured every 5 s using the 40x oil immersion objective of a Nikon TE 300 inverted microscope connected to a software-controlled (Metafluor, Molecular Devices, Sunnyvale, CA, USA) cooled charge coupled (CCD) camera (Sensicam PE, PCO, Kelheim, Germany). Cells were excited during 150-300 ms by a Xenon lamp (100 W, Nikon, Champigny-sur-Marne, France) using a 440/20BP filter and a 455LP dichroic mirror. Dual emission imaging was performed using an Optosplit II emission

splitter (Cairn Research, Faversham, UK) equipped with a 495LP dichroic mirror and BP filters 470/30 (CFP) and 535/30 (YFP), respectively. Spectral bleed-through into the YFP channel was subtracted using the formula: YFP_{corr}=YFP-0.6xCFP. The concentration-effect curves of Iso on cAMP levels were fitted using the equation $Y=A+(E_{max}-A)/(1+10^{((Log EC_{50}-X)))}$ were EC_{50} is the apparent potency, E_{max} the maximal effect of the agonist, A the minimal % CFP/YFP ratio measured.

Detubulation of ventricular myocytes

Detubulation was achieved either by inducing osmotic shock with the control solution used for the different experiments (external Cs^+-Ringer solution prior to patch-clamp or Ringer solution used for Ca^{2+} transient measurement and FRET imaging) containing formamide (1.5 M) for 15 min as described previously (Kawai *et al.*, 1999; Brette *et al.*, 2002) or by preincubating the cells with control solutions containing 300 µM of imipramine for 15 min followed by washout of the CAD.

T-tubule imaging

After plating on laminin, myocytes were bathed for 5 minutes in a Ringer solution and loaded with the lipophilic membrane marker Di-4-ANEPPS (2 µM in a Ringer solution for 10 min). After washout, T-tubules were examined by using a confocal microscope (TCS SP8, Leica Microsystems, Wetzlar, Germany) with a 63X NA 1.20 water immersion objective and the pinhole set to 1 Airy unit. Di-4-ANEPPS was excited at 478 nm and fluorescence collected between 500 and 750 nm.The center image from each cell was selected for a thresholding analysis using a ImageJ plugin described previously (Heinzel *et al.*, 2002). T-tubules quantification was performed using the ImageJ free software. Images were filtered with a despeckle filter and a median filter, after the background was subtracted with the rolling ball algorithm. The image was then binarized using an auto local threshold, with the Bernsen method (Autothreshold plug-in). The contrast threshold parameter was visually adjusted to ensure the coherence of the binarized image with the original one. A region of interest was defined inside the cell excluding the plasma membrane then a percent area was calculated. This value corresponds to the ratio of the number of white pixels over the size of the region multiplied by 100 and thus, constitutes an index of the T-tubules density.

Statistical analysis

All results are expressed as mean±SD. Statistical analysis was performed using GraphPad Prism software (GraphPad software, Inc., La Jolla, CA, USA). Normal distribution was tested by a Shapiro-Wilk normality test. For normally distributed data, an unpaired *t*-test was performed. We performed unpaired *t*-test to determine statistical significance between two groups. Because the data obtained did not follow a normal distribution, a Kruskal-Wallis followed by a Dunn's *post hoc* test was used to

analyse differences between multiple groups. A Chi^2 test followed by a Fischer exact test was used when appropriate. The F-test for model discrimination was used to analyse differences between the concentration-effect curves. Differences with P-values <0.05 were considered as statistically significant. The number of independent experiments performed is indicated in the figure legends.

Results

Imipramine is more efficient and less toxic than formamide to detubulate adult rat ventricular myocytes

Our initial experiments were designed to examine the structure of the t-tubular system in control and adult rat ventricular myocytes treated with either imipramine or formamide, in order to compare the respective ability of these compounds to produce detubulation. To do so, we stained cell membrane with the lipophilic fluorescent dye Di-4-ANEPPS. Using confocal microscopy, we visualized the indicator which highlighted the cell surface on the periphery and T-tubules in the center of control cells (Figure 1A). We then calculated the percentage of the cell interior occupied by membranes accessible to staining to approximate the T-tubules' density. It represented about 20% of the surface of the control cardiomyocytes (Figure 1B, n=34). In contrast, T-tubules were absent in cells treated with imipramine (n=32, $p<0.001$ *versus* control) while in formamide-treated cells, these invaginations were indeed decreased (n=35, $p<0.001$ *versus* control) but still covered 6% of the total measured area to remain more abundant than in imipramine treated cells (Figure 1B, $p<0.01$). Thus, osmotic shock induces partial detubulation while imipramine removes completely the T-tubular system. Furthermore, formamide treatment severely damaged the cell structure, with only ~40% of the cells conserving a rod-shaped appearance while imipramine had no obvious impact on cell morphology (Figure 2A and B, $p<0.001$ *versus* formamide). These results suggest that unlike imipramine, the osmotic shock induced by formamide damages the cells with a large proportion dying upon treatment. Similarly to what has been described with formamide (Brette *et al.*, 2002), detubulation induced by imipramine remained 2 hours after treatment (data not shown), indicating that it is not reversible (Osman *et al.*, 2016) at least within this time frame. Additionally, when Di-4-ANEPPS was incubated prior to imipramine treatment, a striated pattern remained within the cardiomyocyte (data not shown). Thus, with imipramine, T-tubules form vacuoles detached from the sarcolemma within the cell as observed following the osmotic shock evoked by formamide (Brette *et al.*, 2002).

Imipramine decreases cell capacitance and $I_{Ca,L}$ amplitude in adult rat ventricular mycocytes but not in atrial cells

Using the patch-clamp technique in the whole cell configuration, we observed a diminution of cell capacitance from 184.2±10.8 pF (n=21) to 105.2±6.3 (n=20; $p<0.01$) in cells subjected to imipramine (Figure 3A), indicating a loss of nearly 40% of total membrane. A double-pulse protocol allowed to test biophysical properties of the L-type Ca^{2+} current recorded in control cells or in cardiomyocytes pretreated with imipramine (Figure 3B and C). $I_{Ca,L}$ maximal amplitude measured at 0 mV decreased by ~72% from 1528.7±30.4 pA to 432.2±11.9 pA in detubulated cells confirming enrichment of channels within the T-tubules. Half activation potential was depolarized after imipramine treatment

from -13.8±0.9 mV (n=21) in control to -8.9±1.5 mV (n=20, p<0.01) suggesting altered gating of the channels remaining in the sarcolemma. As expected, reversal potential remained unchanged at +59 mV in all tested conditions. In cells treated with imipramine, half steady-state inactivation potential was slightly but significantly shifted towards negative potentials from -24.9±0.2 mV to -26.9±0.3 mV (n=20-21, p<0.01). Furthermore, in accordance with less Ca^{2+} dependent inactivation (Argibay *et al.*, 1988), at potentials more positive than +20 mV, $I_{Ca,L}$ elicited by the test pulse became progressively larger in cells treated with the antidepressant agent (Figure 3C).

Because the majority of adult rat atrial cardiomyocytes lack t-tubule invaginations (Brette *et al.*, 2002; Smyrnias *et al.*, 2010), we tested the effect of imipramine in these cells for potential side effects. Besides, this allowed us to test whether the diminution of $I_{Ca,L}$ amplitude recorded in imipramine treated ventricular cardiomyocytes could be the consequence of its known inhibitory effect on cardiac $I_{Ca,L}$ at µM concentration (Isenberg & Tamargo, 1985). Unlike in ARVMs, preincubation of atrial myocytes with imipramine followed by washout caused a small but non-significant effect on membrane capacitance (Figure 4A). Furthermore, imipramine preincubation had no significant effect on either amplitude or voltage dependence of $I_{Ca,L}$ in atrial cells (Figure 4B). These results indicate that a 15 min exposure of cardiomyocytes to the cationic amphiphilic drug followed by washout has no direct effect on cell membrane nor on LTCCs.

To determine whether the β-AR stimulation of $I_{Ca,L}$ was affected by imipramine preincubation, ARVMs were subjected to an application of a submaximal concentration of isoproterenol (Iso, 3 nM) and the current recorded using the double-pulse protocol allowing to compare the effect of the non-selective β-AR agonist on biophysical properties of the channels in control and detubulated cells (Figure 5A). Maximal conductance (G_{max}) was increased from 0.16±0.01 pS (n=21) up to 0.21±0.01 pS (n=15, p<0.001) in control cells, leading to a 36% increase of $I_{Ca,L}$ density at 0 mV (n=15, p<0.01) (Figure 5B). Similarly, in detubulated cells, G_{max} was increased from 0.08±0.01 pS (n=20) to 0.13±0.01 pS by Iso (n=15, p<0.01) and $I_{Ca,L}$ density at 0 mV increased by 22% (n=15, p<0.01) (Figure 5B). The difference observed on $I_{Ca,L}$ amplitude elicited by the test pulse in cells treated with imipramine was abolished upon Iso treatment and the half inactivation potential remained hyperpolarized at -26.5±0.3 mV in imipramine treated cells (n=15, p<0.01) compared to -24.5±0.2 mV measured in non-treated cells (Figure 5C).

Effect of imipramine treatment on Ca^{2+} transients and contraction of adult rat ventricular myocytes

To test the consequences of detubulation induced by imipramine on ECC, we recorded calcium transients (CaT) and sarcomere shortening (SS) simultaneously in cells loaded with 1 µM Fura-2 and paced at 1 Hz in control conditions and upon β-adrenergic stimulation (Iso, 3 nM) (Figure 6A).

Cells pre-incubated with imipramine had an average diastolic sarcomere length of 1.80±0.01 µm (n=14) slightly but significantly increased compared to that of control ARVMs 1.68±0.02 µm (n=14, p<0.001). The cationic amphiphilic drug drastically decreased mean CaT amplitude from 30.4±1.6% (n=15) above diastolic Fura-2 ratio in control cells to 8.2±2.6% (n=14, p<0.001) (Figure 6B). SS was 9.7±1.3% of diastolic sarcomere length (n=15) in control ARVMs and was also diminished by the imipramine pre-treatment (2.3±1.3%, n=14, p<0.05) (Figure 6B). In control cells, CaT and SS declined to diastolic levels with average time constants (τ) of 0.18±0.01 s and 0.08±0.01 s respectively (n=15). Decline of CaT was slowed in imipramine treated cells (τ=0.29 ± 0.03 s, n=14) as well as relaxation kinetics (τ=0.43 ± 0.13 s, n=14, p<0.001) (Figure 6C). Strikingly, imipramine decreased the rise velocity of CaT from 35.8±6.6 ratio unit/s (n=15) to 10.8±3.15 ratio unit/s (n=14, p<0.01) and of SS from 2.4±0.3 µm/s (n=15) to 3.9±0.3 µm/s (n=14, p<0.01) (Figure 6D).

In control myocytes, application of a submaximal concentration of Iso (3 nM) slightly increased CaT amplitude and accelerated Ca^{2+} return to diastolic levels (τ=0.1±0.01 ratio unit/s, n=15, p<0.001; Figure 6B and C). Upon Iso, a tendency for acceleration of the rising phase of CaT was observed (57.6±10.3 ratio unit/s, n=15; Figure 5D). The β-AR stimulation produced inotropic effects, increasing SS to 15.9±1.2% (n=15, p<0.05) and slight but not significant lusitropic effects (Figure 6B and C). In cells pre-treated with imipramine, Iso increased CaT amplitude ~2.3-fold (n=14, p<0.05) which remained significantly decreased compared to CaT recorded in control cells exposed to Iso (Figure 6B, n=14, p<0.05). Noticeably, in imipramine treated cells, while Iso increased the rise velocity of SS (n=15, p<0.01) similarly to what was observed in Crtl cells (n=14, p<0.05), it failed to speed up the onset of CaT. However, as expected, the decay of CaT became ~3 times faster (n=14, p<0.0001) and SS relaxation increased 6-fold (n=14, p<0.01) to become similar to those of control cells upon β-AR stimulation (Figure 6C). Another striking effect of imipramine pre-treatment was to favor Ca^{2+} perturbances (Figure 6E). While we did not observe spontaneous Ca^{2+} activities in control cells neither under basal conditions nor upon Iso, more than 40% of the detubulated cells with the antidepressant agent exhibited pro-arrhythmic events (n=15, p<0.01), a proportion reaching nearly 80% upon β-AR stimulation (n=14, p<0.0001 *versus* control cells in Iso).

Effect of Imipramine treatment on intracellular cAMP levels produced upon a β-adrenergic stimulation in adult rat ventricular myocytes

Next, we compared cAMP levels in control ventricular cardiomyocytes and in cells subjected to imipramine pretreatment by overexpressing the FRET-based sensor Epac-S^{H187} (Klarenbeek *et al.*, 2015) in ARVMs using a recombinant adenovirus. As shown in Figure 6A, in a control cell, a brief application of Iso (15 s, 100 nM) increased transiently the CFP/YFP ratio. The mean variation of FRET ratio produced by Iso in control cells was 78.9±6.2 % (n=11) and this was reduced by 27.8%

in cells subjected to imipramine (n=11, p<0.01) (Figure 6B), without any significant alteration in the time course of the signals. We next subjected cells to sustained increasing concentrations of Iso from 1 nM up to 300 nM (Figure 6C). The FRET ratio increased in both conditions, but the plateau value was decreased in detubulated cells (n=17-28, p<0.001). While apparent potency (EC_{50}) remained identical (EC_{50} was 19.6±6.0 nM in control versus 18.3±6.8 nM in imipramine), the maximal effect of Iso was reduced from 105.7±0.1% to 76.9±1% by imipramine. Thus, from these results we can conclude that detubulation with a high concentration of the antidepressant agent imipramine diminishes by ~27% the cAMP production, suggesting that the majority of cAMP production upon a non-selective β-AR stimulation occurs outside the T-tubules.

DISCUSSION

Detubulation of ventricular myocytes with imipramine

Our study confirms that imipramine disrupts T-tubules from the surface membrane, and thus can be used as a new detubulating agent. This new method presents several advantages compared to formamide treatment: First, the cells conserve their rod shape after imipramine pretreatment, suggesting that unlike the detubulation evoked by an osmotic shock, imipramine-induced detubulation preserves cell viability. Additionally, this new detubulation method is more efficient since we did not observe tubular system staining with Di-4-ANEPPS after imipramine treatment while we observed that the interior of the surviving cells after formamide treatment still exhibited few tubules as shown previously (Kawai *et al.*, 1999). More efficient detubulation is further suggested by the ~40% decreased cell capacitance, which is higher than the 26 to 30% diminution produced by formamide in ARVMs that was reported previously (Kawai *et al.*, 1999; Brette & Orchard, 2006; Brette *et al.*, 2006; Bryant *et al.*, 2014). Furthermore, this diminution better approximates the T-tubular membrane fraction (~49%) predicted by computer modeling (Pasek *et al.*, 2008). Besides, since the majority of adult rat atrial myocytes lack T-tubules (Brette *et al.*, 2002; Smyrnias *et al.*, 2010) the absence of a significant effect on cell capacitance allows to exclude any direct effect of imipramine on cell membrane other than detubulation. Another advantage of this new method is that, unlike formamide, imipramine does not detubulate cardiomyocytes by producing an acute osmotic shock, which induces cell volume changes (Kawai *et al.*, 1999) known to evoke electrical remodeling (Ravens, 2003) and signaling pathways activation (Gonano *et al.*, 2014). Imipramine is a tricyclic antidepressant which contains a hydrophobic ring structure and a hydrophilic side chain with a charged cationic amine group, hence it is part of the class term CADs. CADs are one of the largest classes of pharmaceutical compounds and these drugs are known to accumulate at the internal leaflet of cell membranes (Sheetz & Singer, 1974), where they bind to the negative charges of

$PI(4,5)P_2$ via their cationic amine group (Halliwell, 1997). Therefore it constitutes an alternative to the drastic osmotic shock produced by formamide to detubulate cells, interfering with the binding of the phospholipid to BAR domain containing proteins (Suetsugu *et al.*, 2014). However, it is worth noticing that it may interfere with many cellular functions since $PI(4,5)P_2$ not only is crucial for membrane tubulation (Inaba *et al.*, 2016; Hofhuis *et al.*, 2017), but is an actor in endocytosis, exocytosis (Suetsugu S, *et al.,* 2014), regulates ion channels (Royal *et al.*, 2017) and is involved in Ca^{2+} signaling and intracellular pathways (Berridge, 2009). In ventricular myocytes, the bridging integrator 1 (BIN1) is likely to interact with $PI(4,5)P_2$ because it contains a BAR domain and thus, may allow the correct folding of the T-tubules and formation of the dyad (Hong *et al.*, 2014; Fu *et al.*, 2016). However, it is probably not the sole phospholipid binding protein playing this role in heart since dysferlin, which recruits $PI(4,5)P_2$ to shape the t-tubule system in skeletal muscle (Hofhuis *et al.*, 2017), is also expressed in the heart (Han *et al.*, 2007) where it may also participate in such architectural organization. The role of $PI(4,5)P_2$ in the scaffolding of T-tubules of cardiac cells is further supported by our results which demonstrate that a CAD disconnects these invaginations from surface cell membranes. Interestingly, phospholipids are altered in pressure overload hypertrophied hearts (Reibel *et al.*, 1986), in myocardial infarction (Nasa *et al.*, 1997), in the cardiac tissue from mice treated with doxorubicin (Moulin *et al.*, 2015) or catecholamines (Emilsson & Gudbjarnason, 1981). Thus, decreased $PI(4,5)P_2$ within membranes may constitute a link with the decreased density of these invaginations in heart failure (Hong & Shaw, 2017), an hypothesis which requires further work but is supported by our present results.

Effects of imipramine pretreatment on ECC in ventricular myocytes

While detubulation of cells with imipramine reduced by ~40% cell capacitance, we observed a ~72% decrease of $I_{Ca,L}$ amplitude similar to the diminution by 60 to 76% of $I_{Ca,L}$ previously recorded after formamide treatment (Kawai *et al.*, 1999; Brette *et al.*, 2006; Bryant *et al.*, 2014). This is in line with an enrichment of the T-tubules with LTCCs (Kawai *et al.*, 1999). and suggests that T-tubules concentrate ~4 times more channels than the rest of the membrane; this is less than previously estimated, probably due to previous underestimation of cell capacitance using formamide (Kawai *et al.*, 1999; Pasek *et al.*, 2008). Imipramine is well known to inhibit $I_{Ca,L}$ in cardiac cells and this effect was demonstrated to be reversible even at µM concentrations (Isenberg & Tamargo, 1985). The lack of effect on $I_{Ca,L}$ amplitude or its voltage dependence when measured in atrial cells indicates that the direct effect of imipramine on the channel was fully reversed after washout of the drug during our detubulating procedure. This also confirms that the decreased Ca^{2+} entry measured in ventricular cells is due to an effective loss of channels concentrated within the invaginations. Interestingly, $I_{Ca,L}$ activation was significantly shifted toward depolarized voltages after detubulation. This is compatible with channels being more tightly regulated by PKA in T-tubules (Brette *et al.*, 2004a) where caveolin-

3 facilitates basal activity of the kinase (Timofeyev *et al.*, 2013; Bryant *et al.*, 2014) and the localization of LTCCs (Bryant *et al.*, 2018). Besides, voltage dependence of steady-state inactivation was shifted towards negative potentials, suggesting differential regulation of surface membrane and T-tubule $Ca_V1.2$ channels. This may occur via specific association with different variants of auxiliary subunits such as β or α_2-δ which modulates inactivation of LTCCs (Shaw & Colecraft, 2013). Furthermore, at positive potentials, the degree of $I_{Ca,L}$ inactivation which correlates with the Ca^{2+} dependent-inactivation (Argibay *et al.*, 1988) was less pronounced in detubulated cells. This is in accordance with less negative feedback of Ca^{2+} released from the SR on channels in the sarcolemma (Brette *et al.*, 2004b) and the decreased transient amplitude we observed in myocytes pretreated with imipramine. Imipramine pretreatment diminished by two-thirds CaT amplitude and thus decreased SS. This is equivalent to the previously reported ~70% decreased CaT amplitude induced by formamide detubulation (Kawai *et al.*, 1999; Brette *et al.*, 2002; Brette *et al.*, 2004b) and is probably due to the decreased Ca^{2+} entry in the cardiomyocyte and decreased SR Ca^{2+} load in detubulated cells (Brette *et al.*, 2005). Furthermore, the rise velocity of CaT was impaired and detubulated cells exhibited spontaneous CaT and Ca^{2+} alternans confirming that the T-tubules are critical to ensure normal and rapid, synchronized Ca^{2+} release (Brette *et al.*, 2002; Brette *et al.*, 2005; Oyehaug *et al.*, 2013; Caldwell *et al.*, 2014; Frisk *et al.*, 2016). Moreover, the tendency to decreased rate decline of CaT in imipramine treated cells is compatible with decreased Na^+-Ca^{2+} exchange proteins known to localize in the T-tubules (Kieval *et al.*, 1992; Despa *et al.*, 2003) and decreased SERCA2 activity pumping Ca^{2+} back to the SR due to diminished Ca^{2+} concentration gradient. Altogether, our results demonstrate that the cells pretreated with imipramine exhibit the characteristic features of detubulated cells.

Effect of imipramine on β-adrenergic cAMP signaling and regulation of the ECC

FRET imaging revealed a ~27% decrease of intracellular cAMP levels elicited by brief or sustained non-selective β-AR stimulation in imipramine treated cells. This diminution is in line with decreased cAMP production sites by detubulation, due to the loss of β-AR and AC present in the tubular system (Nikolaev *et al.*, 2010; Timofeyev *et al.*, 2013). The rather low impact of detubulation on β-AR-generated cAMP might result from the fact that upon Iso application, cAMP mainly emanates from sarcolemal β_1-ARs which produce highly diffusible signals throughout the cell (Nikolaev *et al.*, 2010), on the contrary to the β_2-ARs which resides within the invaginations (Nikolaev *et al.*, 2010; Timofeyev *et al.*, 2013). Furthermore, the recovery of cAMP signals which depends on phosphodiesterase activities (Leroy *et al.*, 2008) was not impacted by detubulation. This is probably due to the fact that the enzymes remained attached to the vacuoles disconnected from the sarcolemma after imipramine treatment (data not shown). Consequently, the non-selective β-AR stimulation in detubulated cells still increases $I_{Ca,L}$ because the majority of the LTCC at the surface membrane are still coupled to β_1-

AR/AC (Timofeyev *et al.*, 2013). As a result, Iso was able to restore CaT amplitude, thus contraction by increasing not only Ca^{2+} entry but probably also SR Ca^{2+} load by promoting the PKA phosphorylation of phospholamban and consequently SERCA2 activity, which remains in detubulated cells with formamide (Brette *et al.*, 2004a). The noticeable lusitropic effects we observed upon Iso application suggests that it is also the case in imipramine treated cells. However, the rise velocity of CaT was not augmented by Iso in detubulated cells, on the contrary to what was reported in myocytes treated with formamide (Brette *et al.*, 2004a). This discrepancy might be due to the incomplete detubulation following the osmotic shock while imipramine removes totally the tubular system. Furthermore, imipramine cells also exhibited Ca^{2+} homeostasis perturbations upon Iso, further underlying the crucial role of T-tubules to obtain rapid and synchronized CICR, even upon β-AR stimulation.

CONCLUSIONS

Although the concentration of imipramine we used here to detubulate cardiomyocytes is much higher than the plasmatic levels reached with therapeutic doses (~1 µM), our results suggest that a disorganization of T-tubules may contribute to the clinical cardiotoxic effects of the antidepressant drug, especially upon overdoses (Marshall & Forker, 1982). Indeed it can evoke heart failure in dog (Lucas CM et al., 1992) and intoxication with this TCA has been associated to cardiac arrhythmias, depression of myocardial contractility, hypotension and cardiac arrest (Marshall & Forker, 1982) which might have been caused at least partly, by the detubulation of the cardiomyocytes. Furthermore, besides providing new potential insights into the cardiotoxicity of high doses of imipramine, our results validate a new alternative detubulation technique of cardiomyocytes using an agent which is known to interfere with $PI(4,5)P_2$. This method is more efficient than the osmotic shock induced by formamide and importantly has no impact on cell viability but allows to recapitulate the hallmarks of detubulation on ECC. Thus, we propose imipramine as a novel utensil in the toolbox of cardiac physiologists who aim to study the role of T-tubules in cardiac cells.

AUTHOR CONTRIBUTIONS

JL Conceptualized and designed the work, JL, GV and RF elaborated the Drafting of the work. AB, MB, IB, PL, HBM, JL participated to the acquisition, analysis, and interpretation of data for the work. All authors approved the final version of the manuscript, agreed to be accountable for all aspects of the work in ensuring that questions related to the accuracy or integrity of any part of the work are appropriately investigated and resolved. All persons designated as authors qualify for authorship, and all those who qualify for authorship are listed.

FUNDINGS

Our laboratory is a member of the Laboratory of Excellence LERMIT supported by a grant from ANR (ANR-10-LABX-33) under the program “Investissements d'Avenir” ANR-11-IDEX-0003-01. This work was also funded by grant ANR13BSV10003-02 to GV and ANR-15-CE14-0014-01 to RF. AB is the recipient of a PhD fellowship from the French Ministère de l’Enseignement supérieur, de la Recherche et de l’Innovation. MB is the recipient of a PhD fellowship from the LabEX LERMIT and IB was supported by doctoral grants from the CORDDIM program of Région Ile-de-France and the Fondation pour la Recherche Médicale..

ACKNOWLEDGMENTS

We thank Dr. Kees Jalink (Division of Cell Biology, The Netherlands Cancer Institute, Amsterdam, The Netherlands) for sharing the Epac-SH187 FRET-based sensor, Florence Lefebvre for the preparation of the cardiomyocytes and the cell culture, Dr Mika Delphine for skillful advices with the ionoptix® system and the measurements of Ca^{2+} transients and sarcomere shortening.

FIGURE LEGENDS

Figure 1. Imipramine is more potent than formamide to detubulate adult rat ventricular myocytes. (A) Representative confocal images of adult rat ventricular myocytes subjected or not to a 15 min preincubation with either 300 µM imipramine or 1.5 M formamide prior to washout and then stained with the lipophilic dye di-4-ANEPPS. The corresponding fluorescence intensity profile in arbitrary units obtained along the white line on the top images are presented on the graphs bellow each cells. **(B)** Graphs showing the mean percentage of T-tubules within the cells (±SD) evaluated using a technique of "thresholding" and pixel counting. This allowed to calculate the percentage occupied by membrane within a region of interest defined inside the cell (excluding the plasma membrane) which is an index of the T-tubule density. The number of cells obtained from 3 rats is indicated on the graph. Statistical significance using a Kruskal-Wallis followed by a Dunn's post hoc test was used is indicated as ***, $p<0.001$.

Figure 2. Detubulation with imipramine but not with formamide preserves rod-shaped of adult rat ventricular myocytes. (A) Representative field area confocal images of adult rat ventricular myocytes subjected to a 15 min pre-incubation with a control solution without or with 300 µM imipramine or 1.5 M formamide prior to washout. Cells were then stained with the lipophilic dye di-4-ANEPPS. **(B)** A graph showing the mean (±SD) percentage of rod-shaped cardiomyocytes is presented. The number of cells obtained from 3 rats is indicated on the graph. Statistical significance using a Chi^2 test followed by a Fischer exact test is indicated as ***, $p<0.001$.

Figure 3. Effect of imipramine on cell capacitance and $I_{Ca,L}$ measured in adult rat ventricular myocytes. (A) The black bar represents the mean value (±SD) of cell capacitance obtained from 21 control cardiomyocytes, the grey bar the mean capacitance of 20 cells pretreated with 300 µM imipramine for 15 minutes before washout. **(B)** L-type Ca^{2+} currents were elicited using the double-pulse protocol from a holding potential of -50 mV (Inset). Superimposed recordings of $I_{Ca,L}$ obtained during the pre-pulses in control or pretreated with imipramine myocytes are shown. **(C)** Mean variation (±SD) current-voltage (left panels) and steady-state inactivation (right panels) relationships for $I_{Ca,L}$ in control (circles, n=21), imipramine (triangles, n=20) cardiomyocytes, These results were obtained in cells isolated from 5 animals. Statistical significance using an unpaired *t*-test is indicated as *, $p<0.05$ and ***, $p<0.001$ (points that occur after the time point indicated on the curves by the arrows are significant).

Figure 4. Imipramine neither affects cell capacitance nor $I_{Ca,L}$ in rat atrial cardiomyocytes. (A) Mean (±SD) of cell capacitance was measured in control atrial cardiomyocytes (black bar, n=14) or atrial cells pre-treated with imipramine 300 µM for 15 min prior washout (grey bar, n=16). **(B)** Mean (±SD) current-voltage (left panels) and steady-state inactivation (right panels) relationships of $I_{Ca,L}$ elicited using a double-pulse protocol from a holding potential of -50 mV in control (circles, n=14) and imipramine treated (triangles, n=16) cardiomyocytes obtained from 5 rats are shown.

Figure 5. Imipramine does not affect the β-adrenergic stimulation of $I_{Ca,L}$ in rat ventricular cardiomyocytes. (A) Superimposed recordings of $I_{Ca,L}$ obtained during the pre-pulses in control or pretreated with imipramine myocytes upon β-AR stimulation by isoproterenol (Iso, 3 nM) are shown. **(B)** Mean (±SD) current-voltage and **(C)** steady-state inactivation (right panels) relationships of $I_{Ca,L}$ elicited using a double-pulse protocol from a holding potential of -50 mV recorded in under basal conditions (filled symbols, n=20-21) or upon Iso (open symbols n=14-17) in control (circles) and imipramine treated (triangles) cardiomyocytes obtained from 5 rats are presented. Statistical significance using an unpaired *t*-test is indicated as *, $p<0.05$ (points that occur after the time point indicated on the curves by the arrows are significant).

Figure 6. Effect of the detubulation induced by imipramine on ECC in adult rat ventricular myocytes. (A) Representative traces of Ca^{2+} transients and sarcomere shortening in Fura-2 loaded control or imipramine-detubulated ventricular cells paced at 1 Hz. This protocol was repeated under basal conditions (Ctrl), upon β-AR stimulation by isoproterenol (Iso, 3 nM). **(B)** Mean amplitude (±SD) of Ca^{2+} transients (upper graph) and sarcomere shortening (lower graph) in Ctrl (black bars), or imipramine treated cells (gray bars). **(C)** Average relaxation kinetics (±SD) and **(D)** mean (±SD) rise velocity of Ca^{2+} transients (upper graphs) and sarcomere shortening (lower graphs) **(E)** Proportion of cells exhibiting pro-arrhythmic spontaneous and asynchronous Ca^{2+} releases. Number of cells is indicated inside each bar representing the mean of 5 independent experiments. Statistical significance is indicated as: *, $p<0.05$; **, $p<0.01$; ***, $p<0.001$. A Kruskal-Wallis followed by a Dunn's post hoc test was used to analyze Ca^{2+} transients, sarcomere amplitude. Chi^2 test followed by a Fischer exact test to compare the percent of arrhythmic cells.

Figure 7. Effect of imipramine on intracellular cAMP levels upon β-adrenergic stimulation. (A) Representative time course of cAMP levels in a cardiomyocyte expressing the Epac-S^{H187} FRET-based sensor upon a brief β-adrenergic stimulation with isoprenaline (Iso, 15s, 30 nM). CFP/YFP ratio was evaluated by the normalized cyan fluorescent protein (CFP) over yellow fluorescent protein (YFP) ratio emitted upon CFP excitation at 440±20 nM. Pseudo-color images of the CFP/YFP ratio were recorded at the times indicated by the letters on the graphs. Scale bar is 10 µm. **(B)** Mean (±SD) variation with time of the CFP/YFP ratio upon a pulse of Iso measured in control (circles, n=14) and imipramine treated (triangles, n=16) cardiomyocytes. **(C)** Concentration-response curves for the effect of isoprenaline on the CFP/YFP ratio measured in control cells (circles) and imipramine treated cardiomyocytes (triangles) (n=17-28). An unpaired *t*-test was used to test the difference in maximal FRET ratio variation and a F-test to compare the concentration-response curves in both conditions. Data represents the mean ±SD of the number of cells obtained from 5 rats. Statistical significance is indicated as **, $p<0.01$ and ***, $p<0.001$.

REFERENCES

Argibay JA, Fischmeister R & Hartzell HC. (1988). Inactivation, reactivation and pacing dependence of calcium current in frog cardiocytes: correlation with current density. *The Journal of physiology* **401,** 201-226.

Berridge MJ. (2009) Inositol trisphosphate and calcium signalling mechanisms. *Biochim Biophys Acta.* **1793(6)**, 933-40.

Brette F, Despa S, Bers DM & Orchard CH. (2005). Spatiotemporal characteristics of SR Ca(2+) uptake and release in detubulated rat ventricular myocytes. *Journal of molecular and cellular cardiology* **39,** 804-812.

Brette F, Komukai K & Orchard CH. (2002). Validation of formamide as a detubulation agent in isolated rat cardiac cells. *American journal of physiology Heart and circulatory physiology* **283,** H1720-H1728.

Brette F & Orchard CH. (2006). No apparent requirement for neuronal sodium channels in excitation-contraction coupling in rat ventricular myocytes. *Circulation research* **98,** 667-674.

Brette F, Rodriguez P, Komukai K, Colyer J & Orchard CH. (2004a). ß-adrenergic stimulation restores the Ca transient of ventricular myocytes lacking T-tubules. *Journal of molecular and cellular cardiology* **36,** 265-275.

Brette F, Salle L & Orchard CH. (2004b). Differential modulation of L-type Ca^{2+} current by SR Ca^{2+} release at the T-tubules and surface membrane of rat ventricular myocytes. *Circulation research* **95,** e1-7.

Brette F, Salle L & Orchard CH. (2006). Quantification of calcium entry at the T-tubules and surface membrane in rat ventricular myocytes. *Biophysical journal* **90,** 381-389.

Bryant S, Kimura TE, Kong CH, Watson JJ, Chase A, Suleiman MS, James AF & Orchard CH. (2014). Stimulation of ICa by basal PKA activity is facilitated by caveolin-3 in cardiac ventricular myocytes. *Journal of molecular and cellular cardiology* **68,** 47-55.

Bryant SM, Kong CHT, Watson JJ, Gadeberg HC, Roth DM, Patel HH, Cannell MB, James AF & Orchard CH. (2018). Caveolin-3 KO disrupts T-tubule structure and decreases ICa density in mouse ventricular myocytes. *American journal of physiology Heart and circulatory physiology*. 315(5):H1101-H1111.

Caldwell JL, Smith CE, Taylor RF, Kitmitto A, Eisner DA, Dibb KM & Trafford AW. (2014). Dependence of cardiac transverse tubules on the BAR domain protein amphiphysin II (BIN-1). *Circulation research* **115,** 986-996.

Despa S, Brette F, Orchard CH & Bers DM. (2003). Na/Ca exchange and Na/K-ATPase function are equally concentrated in transverse tubules of rat ventricular myocytes. *Biophysical journal* **85,** 3388-3396.

Emilsson A & Gudbjarnason S. (1981). Changes in fatty acyl chain composition of rat heart phospholipids induced by noradrenaline. *Biochimica et biophysica acta* **664,** 82-88.

Frisk M, Ruud M, Espe EK, Aronsen JM, Roe AT, Zhang L, Norseng PA, Sejersted OM, Christensen GA, Sjaastad I & Louch WE. (2016). Elevated ventricular wall stress disrupts cardiomyocyte t-tubule structure and calcium homeostasis. *Cardiovascular research* **112,** 443-451.

Fu Y, Shaw SA, Naami R, Vuong CL, Basheer WA, Guo X & Hong T. (2016). Isoproterenol Promotes Rapid Ryanodine Receptor Movement to Bridging Integrator 1 (BIN1)-Organized Dyads. *Circulation* **133,** 388-397.

Gonano LA, Morell M, Burgos JI, Dulce RA, De Giusti VC, Aiello EA, Hare JM & Vila Petroff M. (2014). Hypotonic swelling promotes nitric oxide release in cardiac ventricular myocytes: impact on swelling-induced negative inotropic effect. *Cardiovascular research* **104,** 456-466.

Halliwell WH. (1997). Cationic amphiphilic drug-induced phospholipidosis. *Toxicol Pathol* **25,** 53-60.

Han R, Bansal D, Miyake K, Muniz VP, Weiss RM, McNeil PL & Campbell KP. (2007). Dysferlin-mediated membrane repair protects the heart from stress-induced left ventricular injury. *The Journal of clinical investigation* **117,** 1805-1813.

Heinzel FR, Bito V, Volders PG, Antoons G, Mubagwa K & Sipido KR. (2002). Spatial and temporal inhomogeneities during Ca^{2+} release from the sarcoplasmic reticulum in pig ventricular myocytes. *Circulation research* **91,** 1023-1030.

Hofhuis J, Bersch K, Bussenschutt R, Drzymalski M, Liebetanz D, Nikolaev VO, Wagner S, Maier LS, Gartner J, Klinge L & Thoms S. (2017). Dysferlin mediates membrane tubulation and links T-tubule biogenesis to muscular dystrophy. *Journal of cell science* **130,** 841-852.

Hong T & Shaw RM. (2017). Cardiac T-Tubule Microanatomy and Function. *Physiological reviews* **97,** 227-252.

Hong T, Yang H, Zhang SS, Cho HC, Kalashnikova M, Sun B, Zhang H, Bhargava A, Grabe M, Olgin J, Gorelik J, Marban E, Jan LY & Shaw RM. (2014). Cardiac BIN1 folds T-tubule membrane, controlling ion flux and limiting arrhythmia. *Nat Med* **20,** 624-632.

Inaba T, Kishimoto T, Murate M, Tajima T, Sakai S, Abe M, Makino A, Tomishige N, Ishitsuka R, Ikeda Y, Takeoka S & Kobayashi T. (2016). Phospholipase Cbeta1 induces membrane tubulation and is involved in caveolae formation. *Proceedings of the National Academy of Sciences of the United States of America* **113,** 7834-7839.

Isenberg G & Tamargo J. (1985). Effect of imipramine on calcium and potassium currents in isolated bovine ventricular myocytes. *Eur J Pharmacol* **108,** 121-131.

Kawai M, Hussain M & Orchard CH. (1999). Excitation-contraction coupling in rat ventricular myocytes after formamide-induced detubulation. *Am J Physiol* **277,** H603-609.

Kieval RS, Bloch RJ, Lindenmayer GE, Ambesi A & Lederer WJ. (1992). Immunofluorescence localization of the Na-Ca exchanger in heart cells. *Am J Physiol* **263,** C545-550.

Klarenbeek J, Goedhart J, van Batenburg A, Groenewald D & Jalink K. (2015). Fourth-generation epac-based FRET sensors for cAMP feature exceptional brightness, photostability and dynamic range: characterization of dedicated sensors for FLIM, for ratiometry and with high affinity. *PloS one* **10,** e0122513.

Leroy J, Abi-Gerges A, Nikolaev VO, Richter W, Lechêne P, Mazet J-L, Conti M, Fischmeister R & Vandecasteele G. (2008). Spatiotemporal dynamics of ß-adrenergic cAMP signals and L-type Ca^{2+} channel regulation in adult rat ventricular myocytes: Role of phosphodiesterases. *Circulation research* **102,** 1091-1100.

Lucas CM, Cheriex EC, van der Veen FH, Habets J, van der Nagel T, Penn OC, Wellens HJ. (1992) Imipramine induced heart failure in the dog: a model to study the effect of cardiac assist devices. *Cardiovascular Research*, **26(8)**:804-9.

Marshall JB & Forker AD. (1982). Cardiovascular effects of tricyclic antidepressant drugs: therapeutic usage, overdose, and management of complications. *American heart journal* **103,** 401-414.

Mika D, Bobin P, Pomerance M, Lechene P, Westenbroek RE, Catterall WA, Vandecasteele G, Leroy J & Fischmeister R. (2013). Differential regulation of cardiac excitation-contraction coupling by cAMP phosphodiesterase subtypes. *Cardiovascular research* **100,** 336-346.

Moulin M, Solgadi A, Veksler V, Garnier A, Ventura-Clapier R & Chaminade P. (2015). Sex-specific cardiac cardiolipin remodelling after doxorubicin treatment. *Biol Sex Differ* **6,** 20.

Nasa Y, Sakamoto Y, Sanbe A, Sasaki H, Yamaguchi F & Takeo S. (1997). Changes in fatty acid compositions of myocardial lipids in rats with heart failure following myocardial infarction. *Molecular and cellular biochemistry* **176,** 179-189.

Nikolaev VO, Moshkov A, Lyon AR, Miragoli M, Novak P, Paur H, Lohse MJ, Korchev YE, Harding SE & Gorelik J. (2010). ß$_2$-Adrenergic receptor redistribution in heart failure changes cAMP compartmentation. *Science* **327,** 1653-1657.

Osman S, Taylor KA, Allcock N, Rainbow RD & Mahaut-Smith MP. (2016). Detachment of surface membrane invagination systems by cationic amphiphilic drugs. *Sci Rep* **6,** 18536.

Oyehaug L, Loose KO, Jolle GF, Roe AT, Sjaastad I, Christensen G, Sejersted OM & Louch WE. (2013). Synchrony of cardiomyocyte Ca(2+) release is controlled by T-tubule organization, SR Ca(2+) content, and ryanodine receptor Ca(2+) sensitivity. *Biophysical journal* **104,** 1685-1697.

Pasek M, Brette F, Nelson A, Pearce C, Qaiser A, Christe G & Orchard CH. (2008). Quantification of t-tubule area and protein distribution in rat cardiac ventricular myocytes. *Progress in biophysics and molecular biology* **96,** 244-257.

Ravens U. (2003). Mechano-electric feedback and arrhythmias. *Prog Biophys & Mol Biol* **82,** 255-266.

Reibel DK, O'Rourke B, Foster KA, Hutchinson H, Uboh CE & Kent RL. (1986). Altered phospholipid metabolism in pressure-overload hypertrophied hearts. *Am J Physiol* **250,** H1-6.

Royal AA, Tinker A, Harmer SC. (2017) Phosphatidylinositol-4,5-bisphosphate is required for KCNQ1/KCNE1 channel function but not anterograde trafficking. *PLoS One* **12(10)**:e0186293.

Shaw RM & Colecraft HM. (2013). L-type calcium channel targeting and local signalling in cardiac myocytes. *Cardiovascular research* **98,** 177-186.

Sheetz MP & Singer SJ. (1974). Biological membranes as bilayer couples. A molecular mechanism of drug-erythrocyte interactions. *Proceedings of the National Academy of Sciences of the United States of America* **71,** 4457-4461.

Smyrnias I, Mair W, Harzheim D, Walker SA, Roderick HL & Bootman MD. (2010). Comparison of the T-tubule system in adult rat ventricular and atrial myocytes, and its role in excitation-contraction coupling and inotropic stimulation. *Cell calcium* **47,** 210-223.

Suetsugu S, Kurisu S & Takenawa T. (2014). Dynamic shaping of cellular membranes by phospholipids and membrane-deforming proteins. *Physiological reviews* **94,** 1219-1248.

Timofeyev V, Myers RE, Kim HJ, Woltz RL, Sirish P, Heiserman JP, Li N, Singapuri A, Tang T, Yarov-Yarovoy V, Yamoah EN, Hammond HK & Chiamvimonvat N. (2013). Adenylyl cyclase subtype-specific compartmentalization: differential regulation of L-type Ca2+ current in ventricular myocytes. *Circulation research* **112,** 1567-1576.

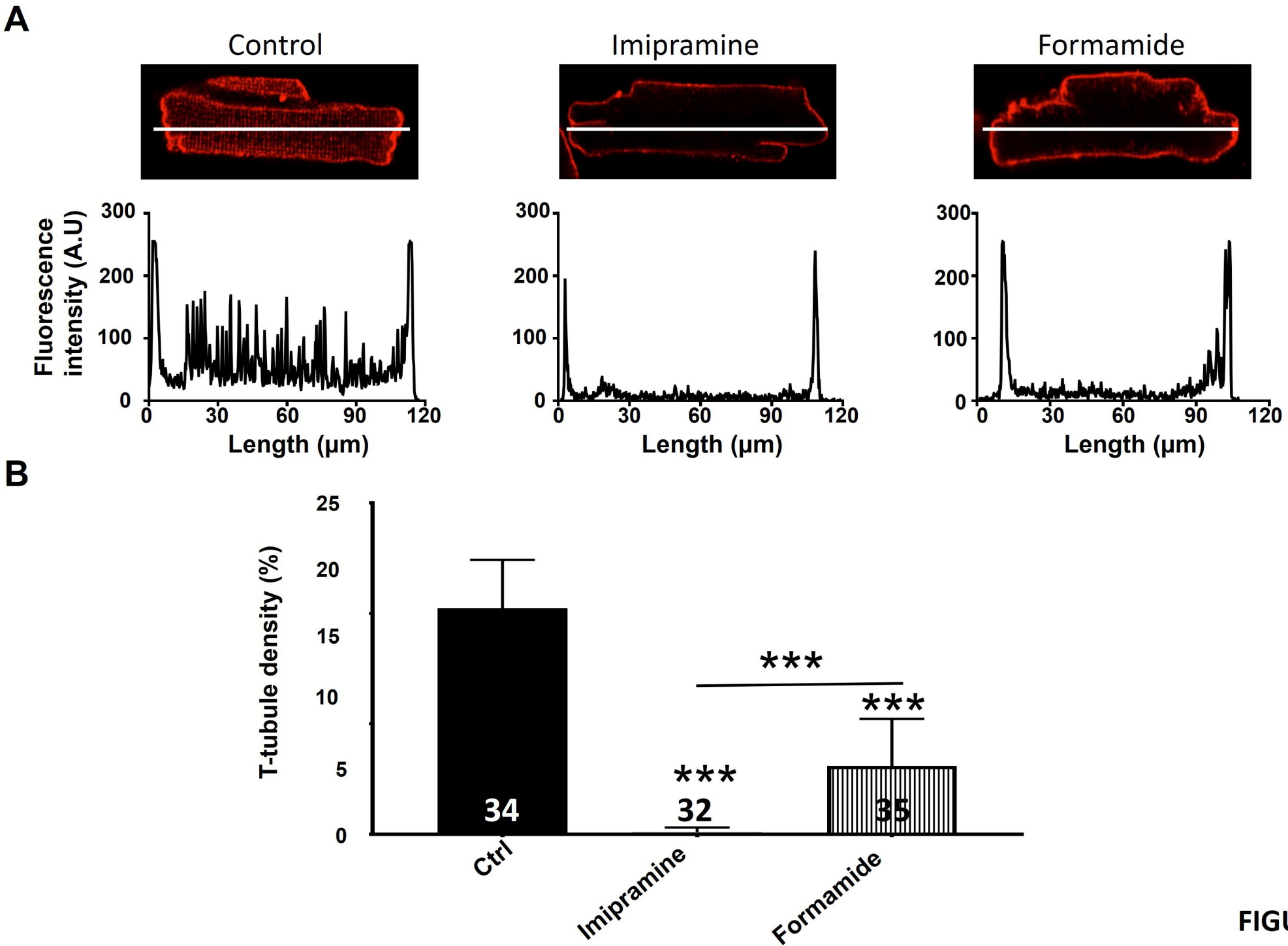
A
Control
Imipramine
Formamide
Fluorescence intensity (A.U)
300
200
100
0
0
30
60
90
120
Length (µm)
B
T-tubule density (%)
25
20
15
10
5
0
34
32
35
***
***
***
Ctrl
Imipramine
Formamide

FIGURE 1

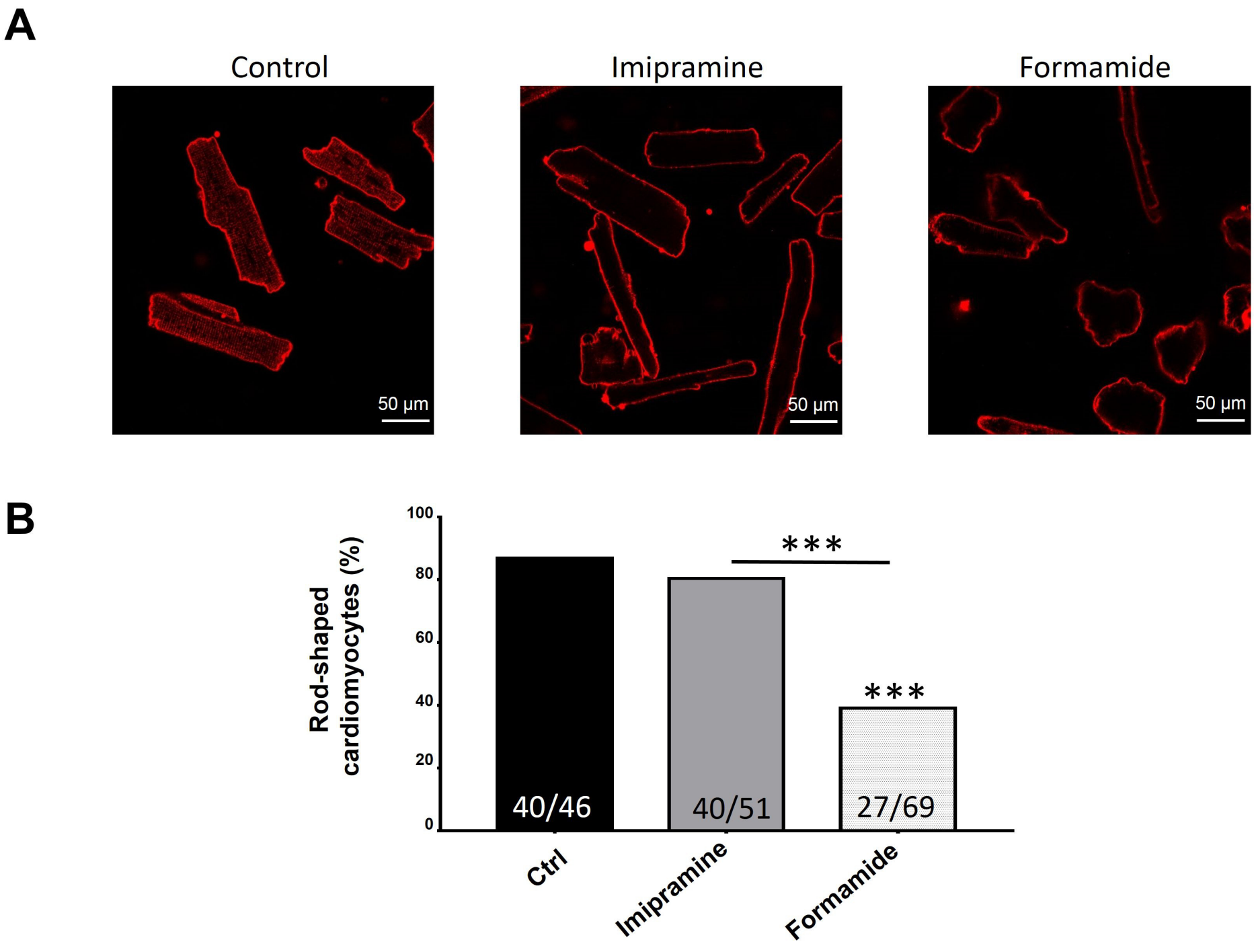
A
Control
Imipramine
Formamide
50 µm
50 µm
50 µm
B
Rod-shaped cardiomyocytes (%)
100
80
60
40
20
0
***
***
40/46
40/51
27/69
Ctrl
Imipramine
Formamide

FIGURE 2

FIGURE 3

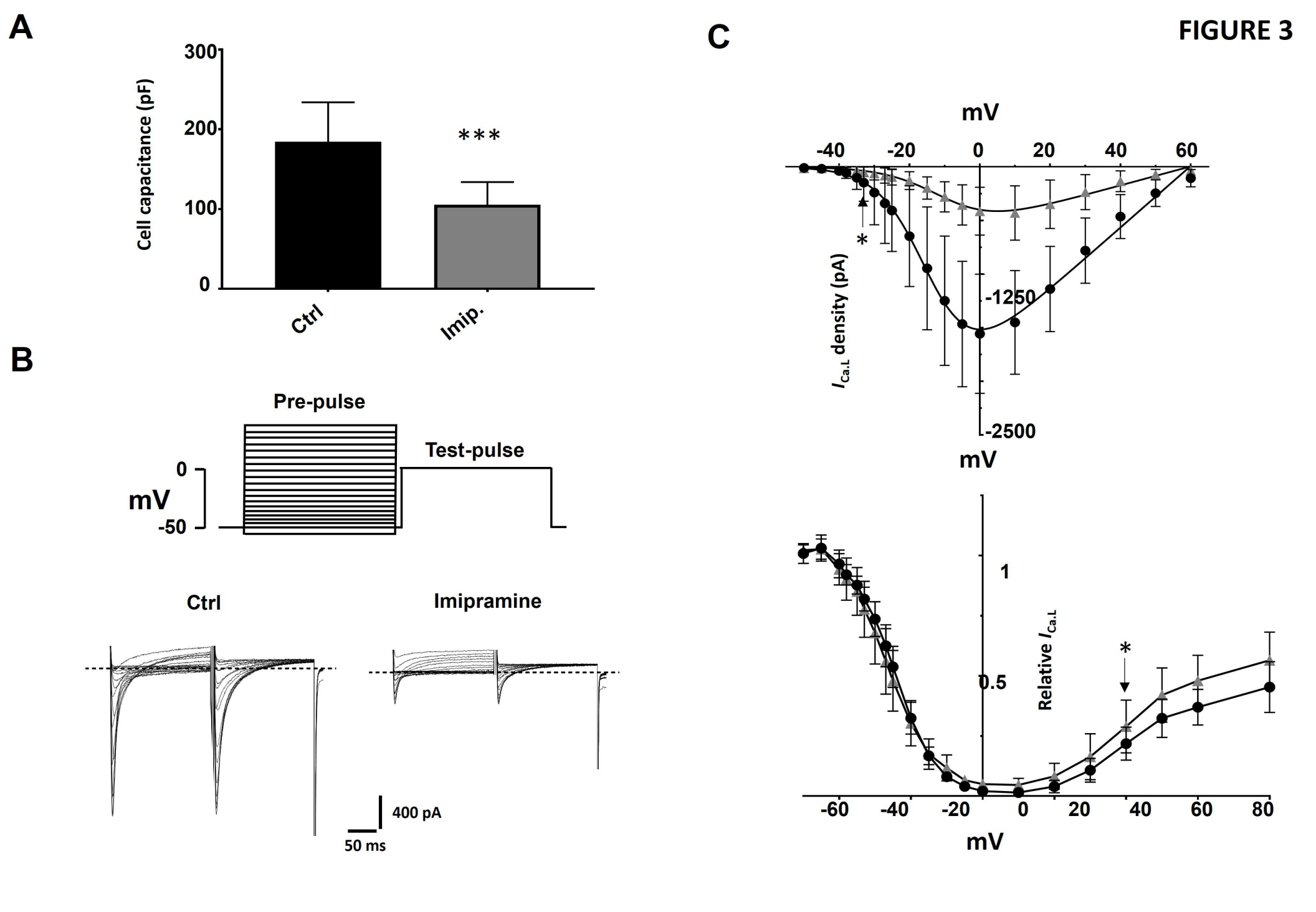
A
300
200
100
0
Cell capacitance (pF)
***
Ctrl
Imip.
B
Pre-pulse
Test-pulse
0
mV
-50
Ctrl
Imipramine
400 pA
50 ms
C
mV
-40
-20
0
20
40
60
*
-1250
-2500
$I_{Ca.L}$ density (pA)
mV
1
0.5
Relative $I_{Ca.L}$
*
-60
-40
-20
0
20
40
60
80
mV

FIGURE 4

A

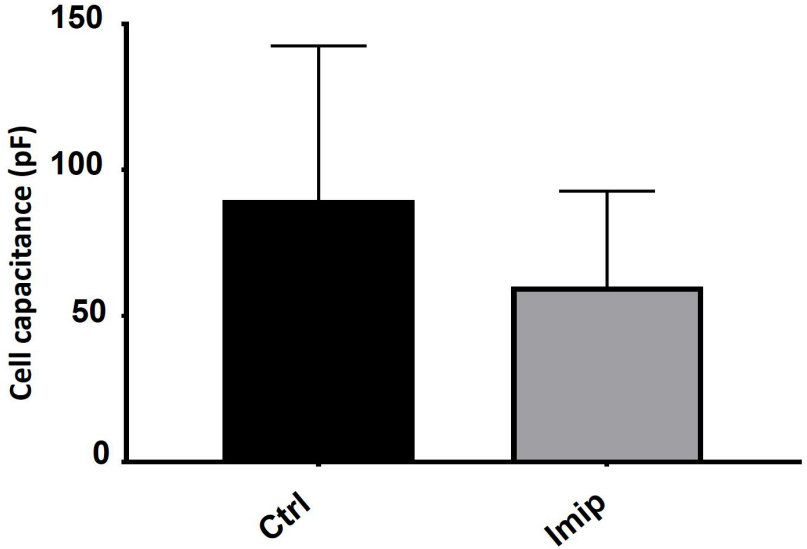

B

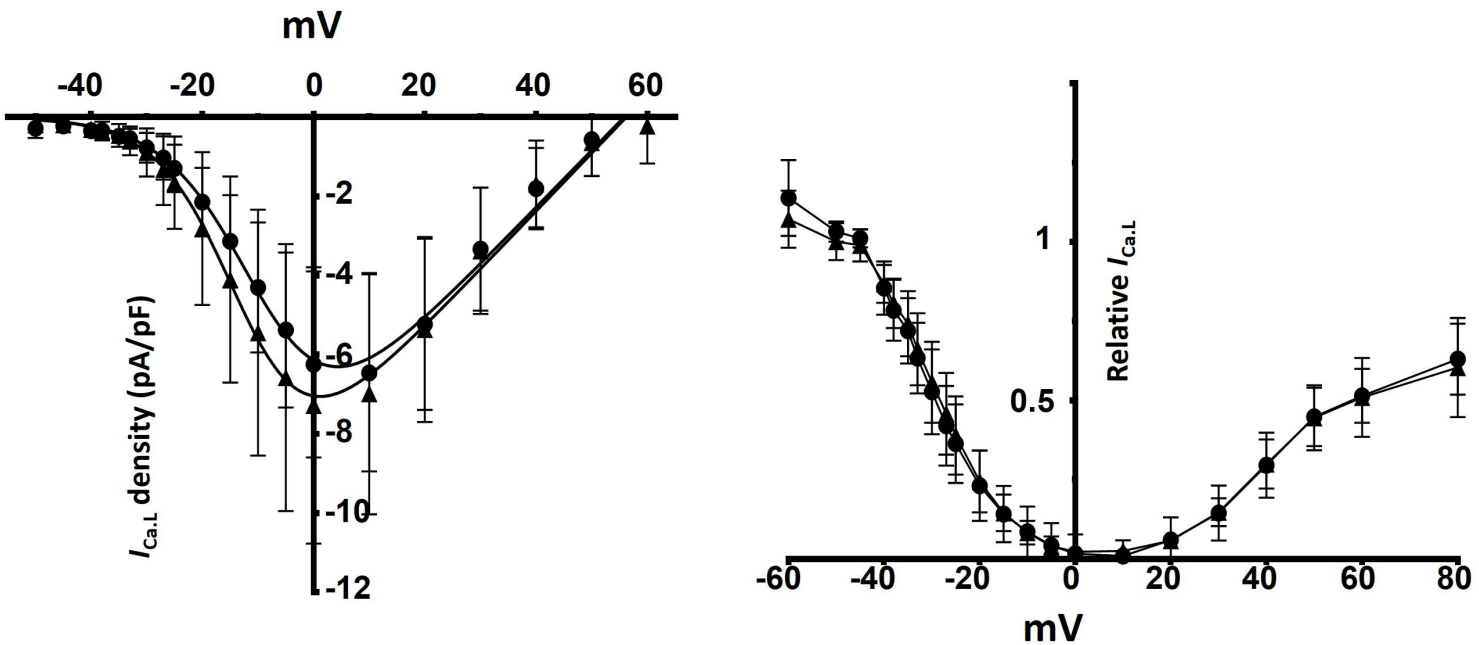

n=14-16. N=5

FIGURE 5

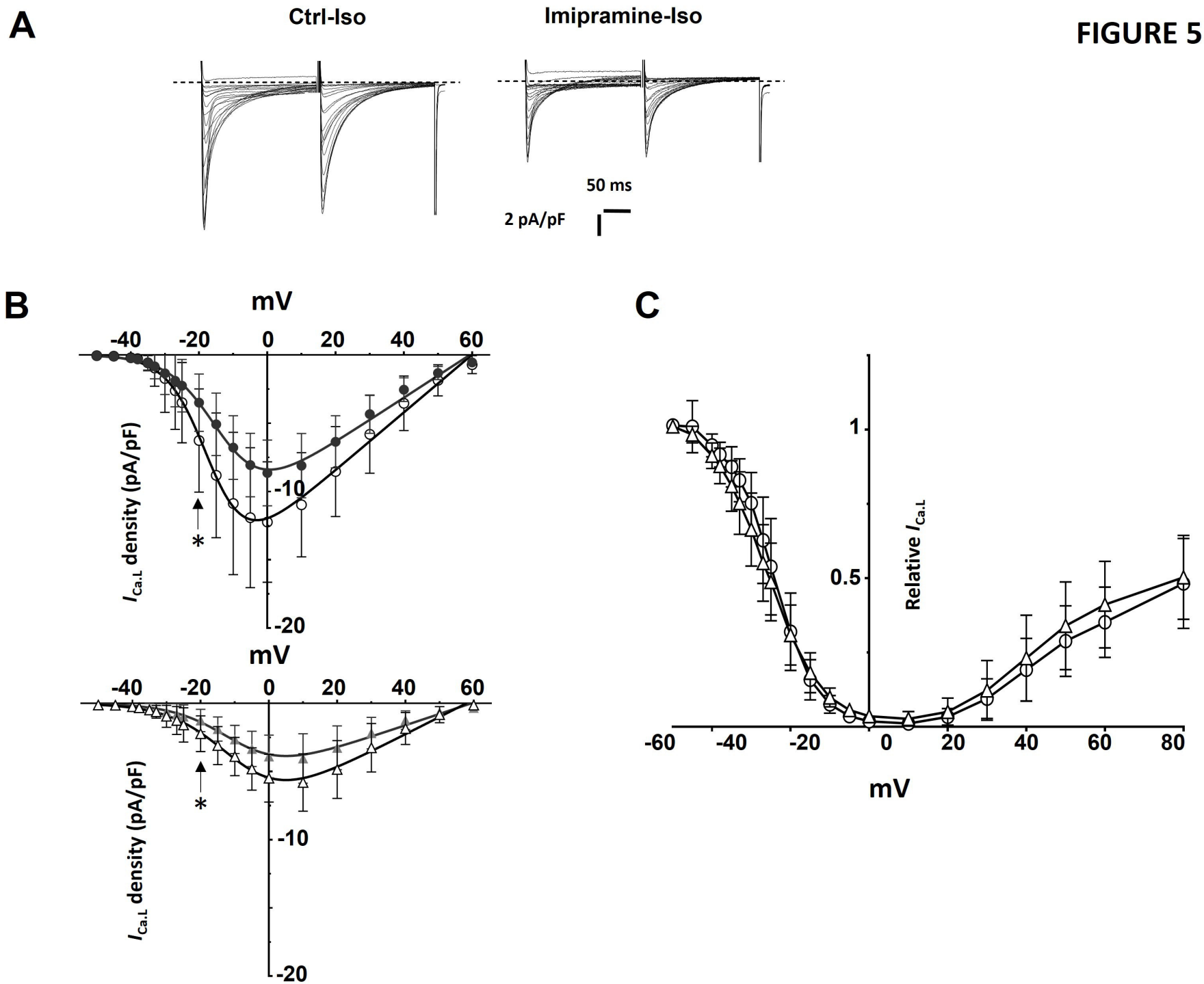
A
Ctrl-Iso
Imipramine-Iso
50 ms
2 pA/pF
B
mV
-40
-20
0
20
40
60
-10
-20
$I_{Ca.L}$ density (pA/pF)
*
mV
-40
-20
0
20
40
60
-10
-20
$I_{Ca.L}$ density (pA/pF)
*
C
1
0.5
Relative $I_{Ca.L}$
-60
-40
-20
0
20
40
60
80
mV

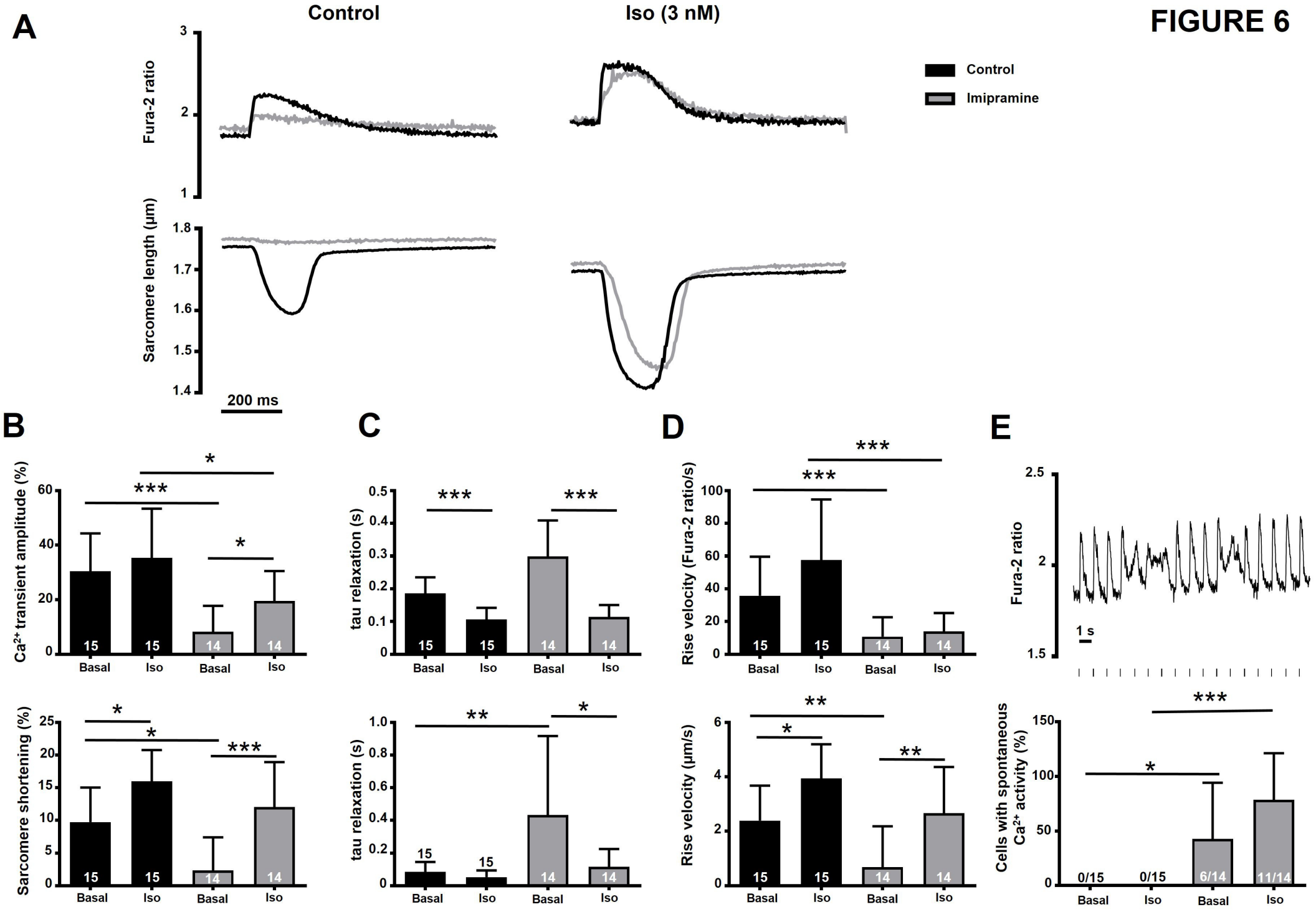
FIGURE 6
A
Control
Iso (3 nM)
Control
Imipramine
Fura-2 ratio
Sarcomere length (µm)
200 ms
B
C
D
E
Ca2+ transient amplitude (%)
tau relaxation (s)
Rise velocity (Fura-2 ratio/s)
Fura-2 ratio
1 s
Sarcomere shortening (%)
tau relaxation (s)
Rise velocity (µm/s)
Cells with spontaneous Ca2+ activity (%)
0/15
0/15
6/14
11/14
Basal
Iso

FIGURE 7

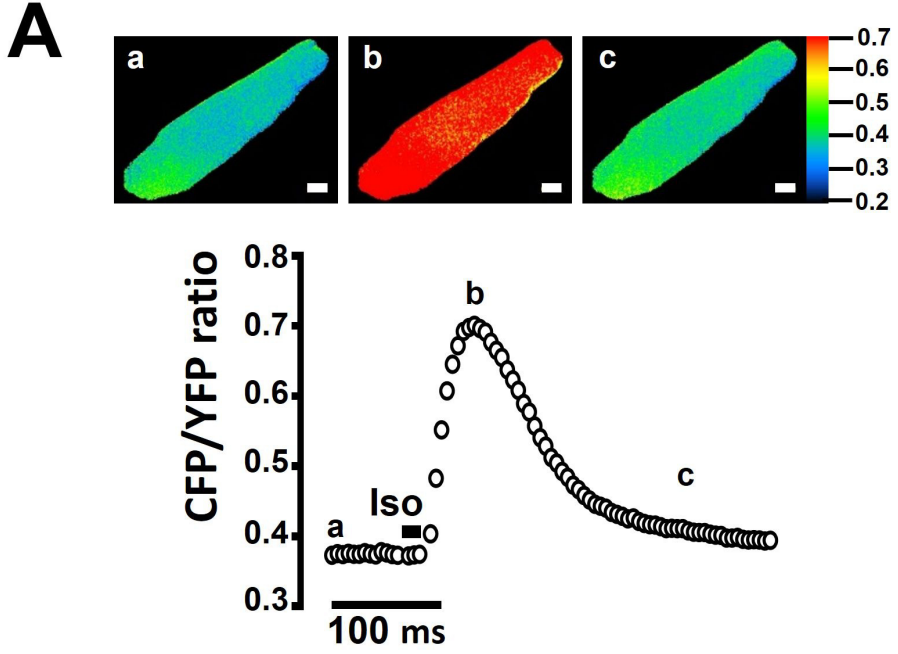
A
a
b
c
0.7
0.6
0.5
0.4
0.3
0.2
CFP/YFP ratio
0.8
0.7
0.6
0.5
0.4
0.3
Iso
100 ms

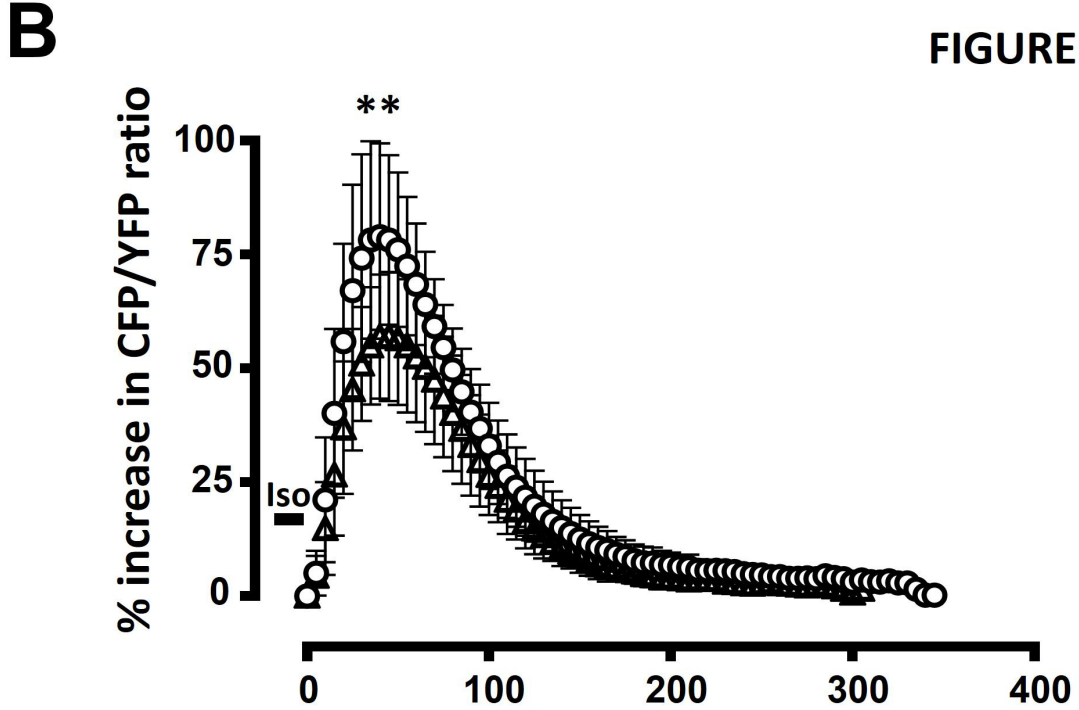
B
% increase in CFP/YFP ratio
100
75
50
25
0
**
Iso
0
100
200
300
400

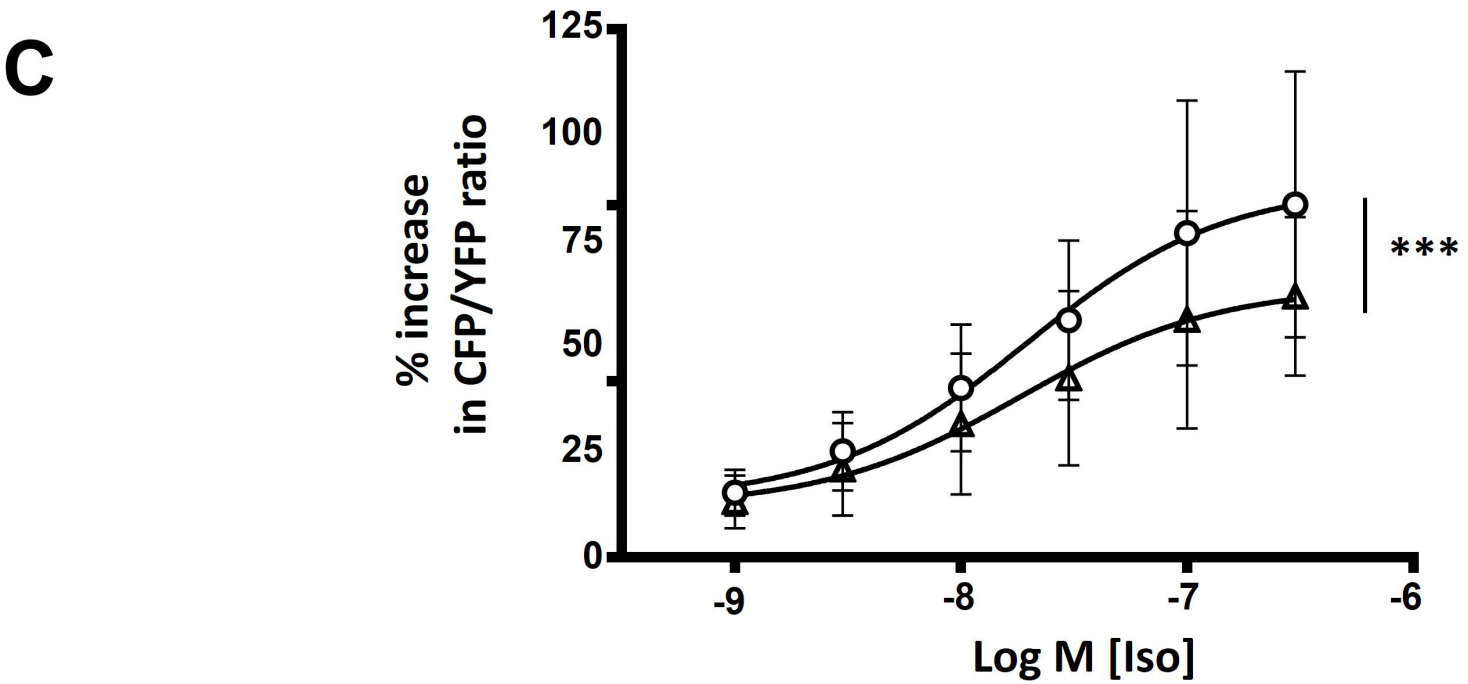
C
% increase
in CFP/YFP ratio
125
100
75
50
25
0
***
-9
-8
-7
-6
Log M [Iso]